Water Science and Engineering, 2009, 2(3): 96-109
doi:10.3882/j.issn.1674-2370.2009.03.010

http://kkb.hhu.edu.cn
e-mail: wse@hhu.edu.cn

Experimental study and simulations of infiltration in evapotranspiration landfill covers

Wen-xian ZHANG*[1, 2], Zhan-yu ZHANG[2], Kang WANG[3]

1. College of Water Conservancy and Hydropower Engineering, Hohai University, Nanjing 210098, P. R. China
2. Tibet Agriculture and Animal Husbandry College, Linzhi 860000, P. R. China
3. State Key Laboratory of Water Resources and Hydropower Engineering Science, Wuhan University, Wuhan 430072, P. R. China

Abstract: Various cover systems have been designed for landfill sites in order to minimize infiltration (percolation) into the underlying waste. This study evaluated the soil water balance performance of evapotranspiration covers (ET covers) and simulated percolation in the systems using the active region model (ARM). Experiments were conducted to measure water flow processes and water balance components in a bare soil cover and different ET covers. Results showed that vegetation played a critical role in controlling the water balance of the ET covers. In soil profiles of 60-cm depth with and without vegetation cover, the maximum soil water storage capacities were 97.2 mm and 62.8 mm, respectively. The percolation amount in the bare soil was 2.1 times that in the vegetation-covered soil. The ARM simulated percolation more accurately than the continuum model because it considered preferential flow. Numerical simulation results also indicated that using the ET cover system was an effective way of removing water through evapotranspiration, thus reducing percolation.

Key words: *active region model; evapotranspiration cover; percolation control; water balance*

1 Introduction

The soil cover (i.e., the top layer) is one of the key components of a landfill system. Covers of traditional landfills, which are formed from compacted clay, man-made materials, or a combination of compacted clay and man-made materials, serve as a barrier to minimize the amount of precipitation that enters the landfill and eventually the groundwater system. Resistive barriers rely on low hydraulic conductivity to minimize the movement of water into the underlying waste. However, previous studies have shown that many landfill covers, particularly compacted clay layers, leak because of preferential flow paths caused by desiccation (Khire et al. 1997; Melchior 1997; Gee et al. 2002; Albright et al. 2003). An ET cover relies on vegetation to increase the water storage capacity within the cover. The

This work was supported by the National Natural Science Foundation of China (Grant No. 50609019), the National Basic Research Program of China (the 973 Program) (Grant No. 2006CB403404), and the National Natural Science Foundation of Tibet.
*Corresponding author (e-mail: *vwxmsx@tom.com*)
Received Apr. 2, 2009; accepted Jul. 29, 2009

vegetation plays an essential role in the ET cover system, which allows water to move upward so that downward percolation is negligible or zero.

Field investigation of ET cover systems in Oregon, California, Montana, and Nebraska in the USA have shown that the systems can effectively control percolation in arid and semi-arid areas (Nyhan et al. 1990; Hauser et al. 2001; Albright et al. 2004; Nyhan 2005). Results of ET cover system experiments conducted in New Mexico confirmed that the systems held 99% of rainfall infiltration. A study of an ET cover system in Texas by Scanlon et al. (2003) also showed that evapotranspiration was the key factor in the water balance within the cover soil and increasing vegetation coverage speeded up the decrease of soil moisture. Albrecht and Benson (2001) investigated the possibility of utilizing ET cover systems in semi-humid areas.

Preferential flow is common in natural unsaturated soils. It causes the water to propagate quickly to significant depths, bypassing a large portion of the soil volume. It has been reported that the amount of water percolation across the cover can reach 60% of the total precipitation and the high penetration rate is attributable to preferential flow pathways caused by dry cracking and animal burrows (Khire et al. 2000). Therefore, preferential flow through the soil cover layer causes most of the deep percolation in the system. Without considering preferential flow in the soil, many numerical models and methodologies have generally predicted a significantly lower amount of percolation through landfill covers (Khire et al. 1997; Sadek et al. 2007). The continuum approach (which uses the Richards equation) treats soil water flow as a homogeneous movement of water in the porous media; it therefore usually fails to capture the preferential flow paths. The continuum model may underestimate the landfill percolation. In recent years, the ARM (Liu et al. 1998, 2003), which incorporates fractal flow patterns into the continuum approach, has been developed to characterize preferential water flow in the unsaturated zone. In this study, the ARM was used to simulate soil water dynamics in the ET covers.

The objectives of this study were to investigate the soil water balance performance of ET cover systems and to simulate soil water dynamics and percolation in the ET covers using the ARM.

2 Materials and methods

Six different ET cover designs (six plots) were installed at the Irrigation and Drainage Experimental Station of Wuhan University. The surface area of each plot was 1.3×3.6 m^2 and the cover materials consisted of 0.2-m topsoil (sandy loam with a bulk density of 1.4 g/cm^3), with 0.4-m underlying compacted soil (the same soil texture as the top layer but with a bulk density of 1.65 g/cm^3). The contents of sand, silt, and clay of the soil were 38.4%, 43.6%, and 18.0%, respectively. In every plot, three leachate collectors were set up (each with an area of 30×30 cm^2) between the soil cover layer and the solid waste layer, a micro-lysimeter was installed to measure evapotranspiration, tension meters were embedded at different depths for estimating soil water flux, and TDR (time domain reflectometer) sensors were used at the

same depths to monitor soil water storage changes (Fig. 1). Meteorological parameters, including precipitation, solar radiation, air temperature, relative humidity, and wind speed, were collected every 30 minutes at an automated meteorological station. Vegetation coverage and leaf area index were measured periodically. The experiment was carried out from May 2006 to March 2007.

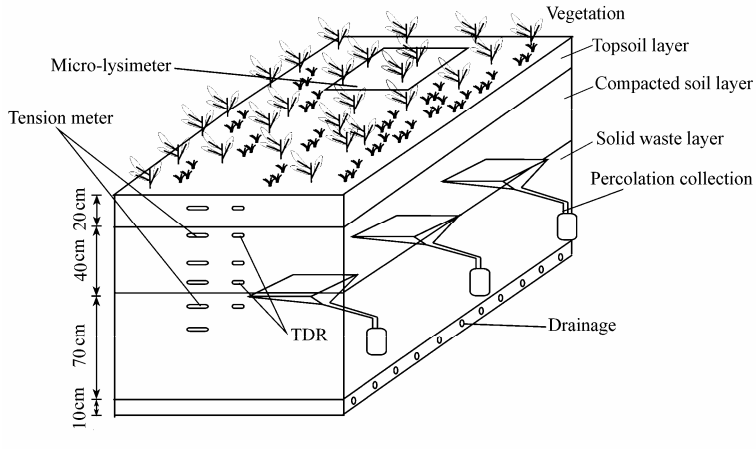

Fig. 1 Diagram of ET cover experimental setup

The surface of Plot 1 was bare soil during the experimental period. In Plots 2, 3, 5, and 6, the topsoil was drill-seeded in April with a mixture of native plants (*Vicia sativa* and *Eragrostis pilosa*). The plant mix (Table 1) was composed of acceptable native vegetation that would provide adequate coverage during both the warm and cool growing seasons. In Plot 3, the installed cover system consisted of three layers from top to bottom: (1) a topsoil layer, (2) a compacted soil layer with a thickness of 20 cm, and (3) a sand drainage layer. The lower drainage layer was composed of 20 cm of clean sand. In Plot 4, a small shrub and local summer grass (*Medicago hispida* and *Avena fatua*) were transplanted in April. In Plot 6, a water-absorbent agent (a super-absorbent polymer) was mixed with the cover soil (in a ratio of 1 g of polymer to 1000 g of dry soil) to increase the soil water-holding capacity. The water-absorbent agent used in this study had the capacity to absorb 200 times more water than its own volume.

Table 1 Structure designs of various ET cover experimental plots

Plot number	Experimental design				Average leaf area index
	Cover thickness (cm)		Coverage of vegetation* (%)		
	Topsoil	Loam	Grass	Shrub	
Plot 1	20	40	0	0	0.09
Plot 2	20	40	50	50	1.76
Plot 3	20	20	100	0	1.86
Plot 4	20	40	100	0	2.17
Plot 5	20	40	75	25	1.47
Plot 6	20	40	50	50	1.40

Note: * refers to the approximate percentage of vegetation each given area.

3 Mathematical model description

Because of the spatial variability and nonlinearity of unsaturated porous media, soil water flow patterns show high heterogeneity, and water flows only in the active region, bypassing the inactive region. Water flow patterns can be characterized as fractal (Hatano and Booltink 1992; Olsson et al. 2002; Wang et al. 2006). Fig. 2 represents grid blocks containing active regions, and their corresponding flow patterns are fractal. In this case, only a portion of the medium within a grid block contributes to water flow. This is conceptually consistent with the preferential flow process. It should be pointed out that, in Fig. 2, a box is shadowed if it covers the active region.

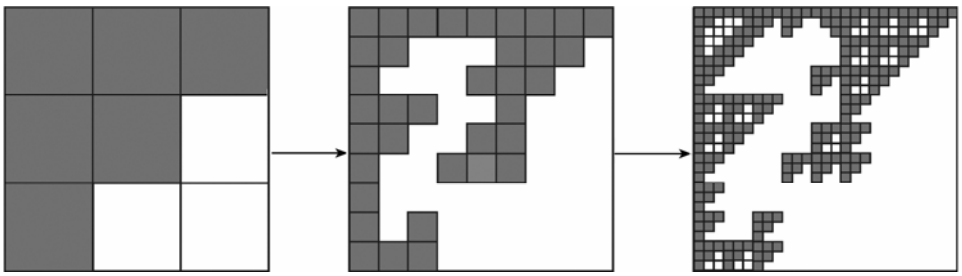

Fig. 2 Illustration of water flow patterns in ARM

Combining the fractal theory and the number of grids of a characteristic size l in the active region yields

$$N(l)=\left(\frac{L}{l}\right)^{D} \tag{1}$$

where $N(l)$ is the number of grids in the active region, L is the size of the whole domain under consideration, and D is the fractal dimension. In Euclidean geometry, the number of grids with size l in the two-dimensional regions is

$$N^{*}(l)=\left(\frac{L}{l}\right)^{E} \tag{2}$$

where $N^{*}(l)$ is the number of grids in the whole region (including active and inactive regions), and E is the Euclidean dimension. Combining Eqs. (1) and (2) gives

$$N(l)^{1/D}=N^{*}(l)^{1/E} \tag{3}$$

The average effective water saturation throughout the whole region S_{e} with a size l can be expressed as

$$S_{\mathrm{e}}=\frac{V}{N^{*}(l)l^{E}} \tag{4}$$

where V is the total water volume in the soil. Similarly, the average effective water saturation in the active region S_{b} (or the areas with gray grids in Fig. 2) is

$$S_{\mathrm{b}}=\frac{V}{N(l)l^{E}} \tag{5}$$

There is a scale $l_1 < L$ satisfying the following condition:

$$V = l_1^E \tag{6}$$

Because a fractal is similar at different scales (Fig. 2), the procedure for deriving Eq. (7) from a grid block with size l can be applied to gray grids with the smaller size of l_1. In this case, for a given grid size smaller than l_1, the number of gray grids is counted as an average number for those within the (previously gray) grids with a size of l_1. Based on Eqs. (1) through (6), the average effective water saturation S_{b1} with the scale l_1 in the gray areas is

$$S_{b1} = \left(S_e\right)^{D/E} \tag{7}$$

According to the fractal theory, if the grid size $l_2 < l_1$ in the active areas of Fig. 2, then the average effective water saturation S_{b2} of the gray areas with a smaller size l_2 is

$$S_{b2} = \left(S_{b1}\right)^{D/E} = \left(S_e\right)^{(D/E)^2} \tag{8}$$

The size of gray grids is further refined and the procedure of Eq. (8) continues for k iterations, at which point all the gray grids cover the active region. In such a case, the water saturation in the active region S_{bk} is as follows:

$$S_{bk} = \left(S_e\right)^{(D/E)^k} \tag{9}$$

Using f to denote the portions of the active region in the whole region, we obtain the following expression based on Eqs. (4) and (5):

$$f = \frac{N(l)}{N^*(l)} = \frac{S_e}{S_{bk}} \tag{10}$$

Combining Eqs. (9) and (10) yields

$$f = \left(S_e\right)^{\gamma} \tag{11}$$

where $\gamma = 1-(D/E)^k$. Eq. (11) is the constitutive relationship of the ARM, which indicates the effective water saturation in the flow domain as a function of f, the fraction of the active region within the entire region. From Eqs. (10) and (11), we have

$$S_{bk} = \frac{S_e}{f} = \left(S_e\right)^{1-\gamma} \tag{12}$$

and

$$S_e = \frac{\theta - \theta_r}{\theta_s - \theta_r} \tag{13}$$

where θ is the average volumetric water content (cm^3/cm^3), and θ_s and θ_r are the saturated volumetric water content (cm^3/cm^3) and residual volumetric water content (cm^3/cm^3), respectively, in the active region. As Liu et al. (2003) proposed, $S_e = fS_{bk}$, and

$$S_{bk} = \frac{\theta_a - \theta_r}{\theta_s - \theta_r} \tag{14}$$

where θ_a is the actual volumetric water content in the active region.

In the continuum model, the capillary pressure head h is characterized as (van

Genuchten 1980)

$$h(S_e)=\frac{1}{\alpha}\left[(S_e)^{-1/m}-1\right]^{1/n} \tag{15}$$

where α, n, and m = 1–1/n are parameters for describing the shape of the soil water retention curve. Accordingly, the soil water characteristic curve in the active region is expressed as follows:

$$h'(S_e)=\frac{1}{\alpha}\left[(S_{bk})^{-1/m}-1\right]^{1/n} \tag{16}$$

Based on Eq. (12), Eq. (16) is rewritten as

$$h'(S_e)=\frac{1}{\alpha}\left[(S_e)^{(\gamma-1)/m}-1\right]^{1/n} \tag{17}$$

In the ARM, the unsaturated hydraulic conductivity of the entire region K has the following form:

$$K = fK_a \tag{18}$$

where K_a refers to the unsaturated hydraulic conductivity in the active region, which can be expressed through the following relationship (van Genuchten 1980):

$$K_a = K_s(S_{bk})^{1/2}\left\{1-\left[1-\left(S_{bk}{}^{1/m}\right)\right]^m\right\}^2 \tag{19}$$

where K_s is the saturated hydraulic conductivity (cm/s). Combining Eqs. (12), (18), and (19), we have

$$K = K_s(S_e)^{(1+\gamma)/2}\left\{1-\left[1-(S_e)^{(1-\gamma)/m}\right]^m\right\}^2 \tag{20}$$

The governing equation for water flow can be characterized by the Richards equation:

$$C\frac{\partial h}{\partial t}=\frac{\partial}{\partial z}\left[K\left(\frac{\partial h}{\partial z}-1\right)\right]-S_r \tag{21}$$

where C is the soil water capacity, t is time, z is the vertical coordinate, and S_r is the amount of root water uptake. Water flow in the ET covers is simulated using Eqs. (17), (20), and (21).

The hydraulic parameters used in the simulation were measured in the lab using soil samples, and the following values were obtained: θ_r=0.036 cm^3/cm^3, θ_s=0.351 cm^3/cm^3, α=0.011 8 m^{-1}, n = 1.762, and $K_s = 2.14\times10^{-4}$ cm/s. The surface boundary was represented by the atmospheric boundary. The bottom boundary was set as the seepage face boundary. Evaporation from the soil surface and transpiration through the plant leaves were estimated using the Penman-Monteith method (Huang 1995):

$$LT=\frac{\frac{P_0}{P}\frac{\Delta}{g}R_{np}+\frac{\rho c_p}{g}\left[e^*(T_a)-e_a\right]\Big/r_{av}}{\frac{P_0}{P}\frac{\Delta}{g}+\left(1+r_{st}/r_{av}\right)} \tag{22}$$

$$LE=\frac{\dfrac{P_0}{P}\dfrac{\Delta}{g}h_{\mathrm{r}}\left(R_{\mathrm{ns}}-G\right)+\dfrac{\rho c_{\mathrm{p}}}{g}\left[h_{\mathrm{r}}e_{\mathrm{s}}^{*}\left(T_{\mathrm{a}}\right)-e_{\mathrm{a}}\right]\Big/r_{\mathrm{av}}}{\dfrac{P_0}{P}\dfrac{\Delta}{g}h_{\mathrm{r}}+\left(r_{\mathrm{s}}/r_{\mathrm{av}}\right)} \tag{23}$$

where L is the latent heat of vaporization, T is the transpiration, E is the evaporation, P is the atmospheric pressure, P_0 is the standard atmospheric pressure, Δ is the slope of saturation vapor pressure curve at air temperature T_{a}, g is the psychometric constant, ρ is the mean air density at constant pressure, c_{p} is the specific heat of the air, $e^{*}(T_{\mathrm{a}})$ is the saturation atmospheric vapor pressure at air temperature T_{a}, $e_{\mathrm{s}}^{*}(T_{\mathrm{a}})$ is the saturation soil vapor pressure at air temperature T_{a}, r_{av} is the aero-dynamic resistance, r_{s} is the bulk surface resistance, r_{st} is the bulk surface resistance describing the resistance of vapor flow through the transpiring crop, h_{r} is the relative humidity in the soil, R_{n} is the incoming solar radiation, R_{np} is the net radiation at the crop surface, R_{ns} is the net radiation at the soil surface, G is the soil heat flux, e_{s} is the saturation vapor pressure, and e_{a} is the actual vapor pressure. The root spatial distributions were estimated according to Vrugt et al. (2001):

$$\beta(z)=\frac{1}{\lambda}\left(1-\frac{z}{z_{\max}}\right)e^{-\frac{1}{\lambda}\frac{p_z}{z_{\max}}\left|z^{*}-z\right|} \tag{24}$$

where $\beta(z)$ is the spatial root distribution with depth, z is the rooting depth, $z_{\max}$ is the maximum rooting depth, z^{*} is the depth at which the maximum $\beta(z)$ was observed (z^{*} = 0.2m), and λ and P_z are empirical parameters. In this study, λ and P_z were set at 1.0, and 2.4, respectively.

Root water uptake may be generalized by introducing a non-uniform distribution of transpiration rate over the root zone:

$$S_{\mathrm{r}}=b(z)L_tT \tag{25}$$

where T is the transpiration (cm/d), L_t is the maximum rooting depth (cm) at time t, and $b(z)$ is the normalized water uptake distribution (1/cm). This function describes the spatial variation of the extraction term S_{r} over the root zone, and is obtained from $b'(z)$ as follows:

$$b(z)=\frac{b'(z)}{\int_{L_t}b'(z)\mathrm{d}L_t} \tag{26}$$

where $b'(z)$ is the prescribed root distribution function. A linear function is used and $b'(z)$ is defined as

$$b'(z)=\frac{1.8}{L_t}-\frac{1.6}{L_t^2}z \tag{27}$$

4 Results and discussion

4.1 Water balance evaluation of ET covers

The efficiency of ET covers in controlling soil moisture and water percolation in the underlying waste was characterized in terms of the water storage capacity and the amount of

evapotranspiration. The relationships between daily precipitation and soil water storage in Fig. 3 show the importance of vegetation in controlling the water balance.

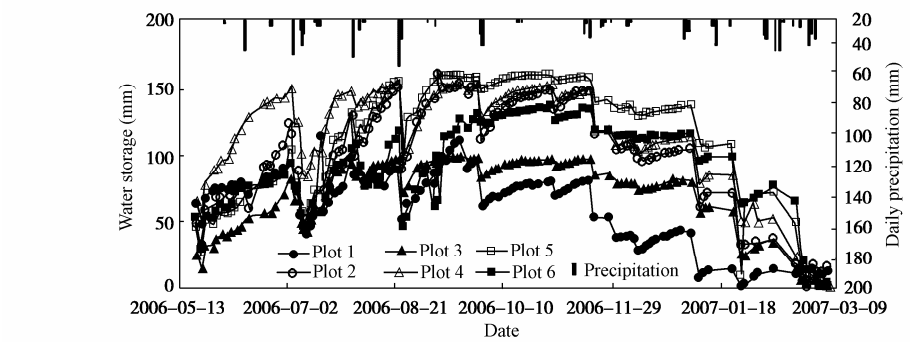

Fig. 3 Daily precipitation and average water storage of each ET cover design

During the summer and autumn of 2006, the average water storage decrease rates (ratio of water storage change to time) of the soil covers were 1.81 mm/d, 2.87 mm/d, 2.30 mm/d, 2.61 mm/d, 2.57 mm/d, and 2.74 mm/d for Plots 1, 2, 3, 4, 5, and 6, respectively. The average decrease rate of the vegetation-covered plots was about 1.45 times of the decrease rate of the bare soil plot (Plot 1). On average, about 100 mm of water was removed from the vegetation-covered plots through evapotranspiration during the summer (from June to August), whereas only 40 mm of water evaporated from the bare soil plot. With the reduced evapotranspiration in the winter, the soil cover water of all plots rose and the water storage decrease rates were slower. In the period from December 2006 to March 2007, the rates were 0.32 mm/d for Plot 1, 0.33 mm/d for Plot 2, 0.30 mm/d for Plot 3, 0.53 mm/d for Plot 4, 0.39 mm/d for Plot 5, and 0.21 mm/d for Plot 6. The results showed that the large decreases in water storage were primarily attributable to the vegetation transpiration.

The average soil moisture changes at depths of 0-20 cm, 20-40 cm, and 40-60 cm are displayed in Figs. 4(a), (b), and (c), respectively. As shown in the figures, the measured water content was highly variable with time at different depths. Temporal variability in water content was greatest near the surface (0-20 cm depth). The variability of soil water content decreased with depth (0.23 cm^3/cm^3 at 0-20 cm depth, 0.14 cm^3/cm^3 at 20-40 cm depth, and 0.10 cm^3/cm^3 at 40-60 cm depth). During the summer and autumn, 20 mm of precipitation penetrated to depths of up to 45 cm in the bare soil plot and up to 30 cm in the vegetation-covered plots.

For the plots with vegetation cover, the average water content ranged from 0.07 cm^3/cm^3 to 0.28 cm^3/cm^3, while for the bare soil plot water content ranged from 0.17 cm^3/cm^3 to 0.34 cm^3/cm^3 during the summer and autumn. As shown in Fig. 3, the soil water content was at its lowest level before the precipitation because of evaporation and transpiration. Sharp increases in water storage occurred after heavy precipitation, and water content reached its maximum

level after precipitation. The maximum soil water storage capacities were 62.8 mm for Plot 1, 90.6 mm for Plot 2, 66.4 mm for Plot 3, 97.2 mm for Plot 4, 80.4 mm for Plot 5, and 64.6 mm for Plot 6. The soil water storage capacity of the plot without vegetation cover was only about 65% of the soil water storage capacity of those with vegetation cover. This shows that the ET covers were highly effective in adjusting the soil water balance of landfill covers.

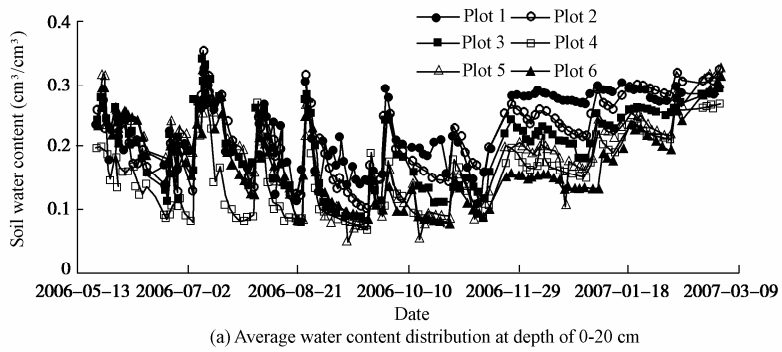

(a) Average water content distribution at depth of 0-20 cm

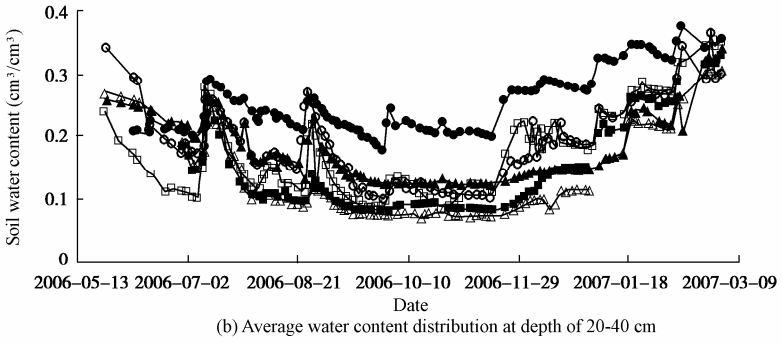

(b) Average water content distribution at depth of 20-40 cm

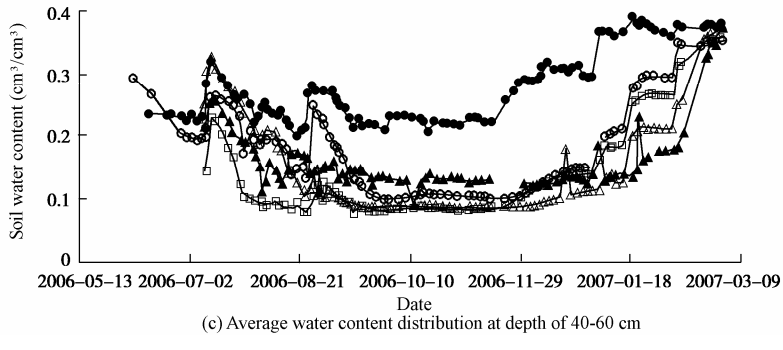

(c) Average water content distribution at depth of 40-60 cm

Fig. 4 Average water content distributions at different depths

As discussed above, the ET cover system adjusted the soil water storage by removing water from within the soil through plant transpiration and soil surface evaporation. Performance of the ET covers was evaluated by monitoring various components of the water balance:

$$ET = P + \Delta W - Q \quad (28)$$

where ET is the amount of evapotranspiration, P is the amount of precipitation (or irrigation), ΔW is the change in soil water storage, and Q is percolation. Various measurement methods were used to monitor the water balance parameters, and ET was calculated through Eq. (28). The relative errors (absolute values) between the calculated and measured ET values ranged from 4% to 14%, indicating that the monitoring systems worked well.

With a total of 563.0 mm of precipitation from June 2006 through March 2007, the percolation process within the upper soil cover layer was closely related to the precipitation process and lagged slightly behind heavy precipitation events. The percolation amount over the study period was less than 15.7% of the precipitation received by all the vegetation-covered plots. In contrast, in the bare soil plot, the percolation amount was 24.2% of the precipitation. With the total rainfall, the smallest amount (48.2 mm) of leachate during the experiment period was observed in Plot 4 (Table 2), which might be attributable to the plot having the largest leaf area index and deep shrub roots. The average leaf area indexes from May to October 2006 were 1.76, 1.86, 2.17, 1.47, and 1.40 for Plots 2, 3, 4, 5, and 6, respectively. The amount of leachate in Plot 6 was also low because of the vegetation cover as well as the water-absorbent agent.

Table 2 Water balance monitoring and calculated results

Plot number	Precipitation (mm)	Moisture changes (mm)	Leachate quantity (mm)	Measured *ET* (mm)	Calculated *ET* (mm)	Ratio* (%)
Plot 1	563.0	−48.6	136.4	406.9	378.0	24.2
Plot 2	563.0	−33.0	71.1	515.8	458.9	12.6
Plot 3	563.0	−20.8	88.7	465.7	453.5	15.7
Plot 4	563.0	−63.6	48.2	482.8	451.2	8.6
Plot 5	563.0	−40.8	64.9	468.1	457.3	11.5
Plot 6	563.0	−48.0	59.6	484.3	475.4	10.5

Note: * refers to the ratio of percolation to precipitation.

Fig. 5 shows the cumulative percolation in the plots. During the summer and autumn months, soil water was removed rapidly through evapotranspiration and evaporation, creating a large water-holding (or storage) capacity in the soil cover. Therefore, the percolation amount was quite low for both vegetation-covered and bare soil plots. For instance, during the period from July 5 to 10, 2006, with a total precipitation of 67 mm, the amount of percolation was 5.8 mm in Plot 1 and the average percolation was only 0.4 mm in the vegetation-covered plots. In the bare soil cover plot, 305 mm of water was removed from the soil, compared with 363 mm on average for the vegetation-covered plots. During the winter months, the soil water storage capacities of both bare and vegetation-covered plots were low. Nevertheless, the soil water content in the vegetation-covered plots was much lower than that in the bare soil plot (Fig. 4). Thus, the soil water storage capacity of the ET covers was larger than that of the bare soil cover, resulting in a smaller amount of percolation. The cumulative precipitation amount was 62 mm from February 27 to March 3, 2007, and the average amount of leachate in plots with and without vegetation covers was 24.0 mm and 46.2 mm, respectively.

The percolation in plots with and without vegetation covers was 11.8% and 24.2% of the total precipitation, respectively.

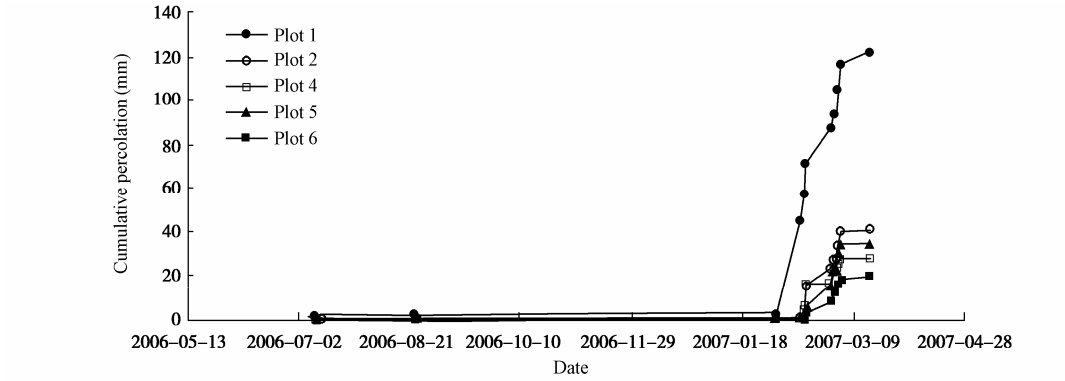

Fig. 5 Measured cumulative percolation in experimental plots of same depth

4.2 Simulation of water flow in landfill covers using ARM

Preferential flow is common in natural unsaturated soils, and it results in quick water propagation to significant depths. Experimental observations in this study also indicated that preferential flow was attributed to percolation. Theoretically, if the cover soil reservoir has enough capacity to store water from precipitation, percolation will not occur. However, we observed percolation during the rainfall periods in most of the plots. The percolation in these plots was attributed to preferential flow through the soil cover layers, which was simulated using the ARM as follows:

The parameter γ in Eq. (11) is key to describing the active regions, ranging from 0 to 1. To determine the γ value, actual infiltration flow patterns were investigated using potassium iodide (KI) as a tracer (Lu and Wu 2003; Hangen et al. 2004). A solution of KI (with a concentration of 20 g/L) was infiltrated into the soil. The infiltrated area was covered with plastic sheets to prevent evaporation and left for 24 hours so that the KI infiltration process could complete. Then, the infiltrated area was removed section by section in the horizontal direction. Each section was smoothed and sprayed with a starch solution (with a concentration of 50 g/L). After spraying, the color changed to blue in the region through which water had passed (the active region). The color-stained patterns were recorded using a digital camera and soil samples were taken in the active regions to measure soil moisture content. The γ value was estimated with Eq. (11) using the measured color stained-patterns and soil water saturation as input information. The estimated γ value was 0.20.

Water content distributions of Plots 1 and 2 were simulated with the ARM and the continuum model to determine how well the simulation matched the measured values. The simulated and measured soil water storage are compared in Fig. 6. In comparison with the ARM, the continuum model overestimated soil water content and, correspondingly, underestimated percolation. The relative error between observed and simulated soil water

content with the continuum model was 19.4%. In contrast, the relative error between observed and simulated soil water content with the ARM model was within 12%.

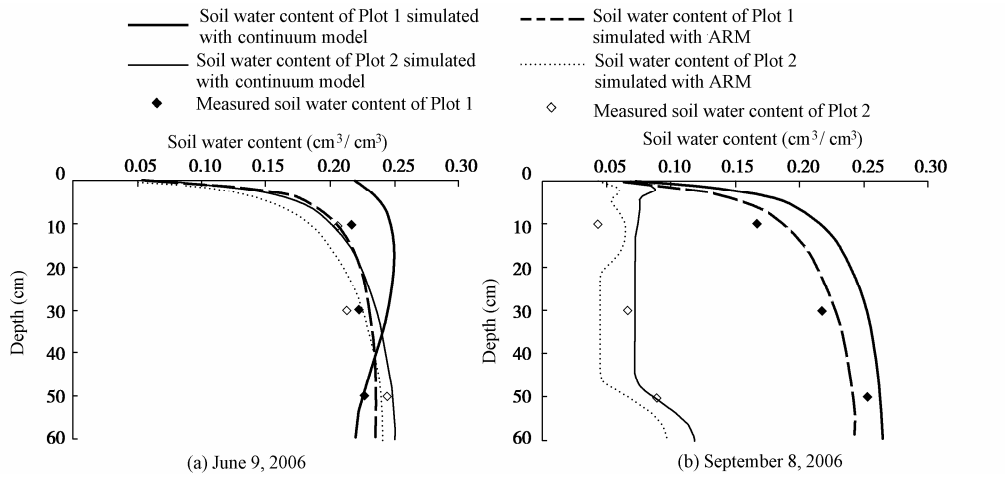

Fig. 6 Numerical comparison between ARM and continuum model

Measured percolation along with the values simulated using the ARM and the continuum model are presented in Table 3. From June 2006 to March 2007, the measured cumulative percolation was 136 mm and 71.1 mm for Plots 1 and 2, respectively. The simulated cumulative percolation using the ARM was 113.9 mm and 61.5 mm for Plots 1 and 2, resulting in relative errors of 16.2% and 13.5%, respectively. The simulated cumulative percolation of the continuum model was 89.6 mm and 51.0 mm for Plots 1 and 2, resulting in relative errors of 34.1% and 28.3%, respectively. Table 3 shows the relative errors of percolation simulated with the ARM and the continuum model in different time periods.

Table 3 Comparison of measured percolation and simulated results with ARM and continuum model

Plot number	Month	Rainfall (mm)	Measured percolation (mm)	Continuum model		ARM	
				Simulated percolation (mm)	Relative error (%)	Simulated percolation (mm)	Relative error (%)
Plot 1	Jun. to Aug.[1)]	214.2	6.1	0	100.0	2.4	60.7
	Sep. to Nov.[1)]	84.0	0	0	0	0	0
	Dec. to Feb.[1)]	190.0	91.3	55.2	39.5	78.7	13.8
	Mar.[2)]	74.8	38.6	34.4	10.9	32.8	15.0
Plot 2	Jun. to Aug.[1)]	214.2	0.6	0	100.0	0	100.0
	Sep. to Nov.[1)]	84.0	0	0	0	0	0
	Dec. to Feb.[1)]	190.0	47.1	24.2	48.6	35.7	24.2
	Mar.[2)]	74.8	23.4	26.8	14.5	25.8	10.3

Note: [1)] indicates 2006; [2)] indicates 2007.

As shown in Fig. 3 and Table 2, during the summer and autumn, cumulative *ET* exceeded infiltration and the soil cover layer provided enough storage to hold precipitation; therefore,

percolation was quite low for both vegetation and bare soil cover plots. In the winter, the soil water content ranged from 0.14 cm^3/cm^3 to 0.30 cm^3/cm^3 for Plot 2 and from 0.23 cm^3/cm^3 to 0.31 cm^3/cm^3 for Plot 1. The measured and ARM-simulated percolations compared favorably for Plots 1 and 2, while the continuum model underestimated percolation significantly.

5 Conclusions

Vegetation plays a critical role in controlling the water balance of the ET covers of landfills. Experimental results for different landfill covers showed that the evapotranspiration amount was 1.5 to 2.8 times that of evaporation from bare soil. In the landfill soil profiles of 60-cm depth with and without vegetation covers, the soil water storage capacities were 97.2 mm and 62.8 mm, respectively. In the ET cover system, the main components of the water balance were evapotranspiration and water storage change. The calculated *ET* values were in good agreement with the micro-lysimeter measured results.

Modeling analysis indicated that the water balance and water content distributions can be simulated fairly well with the ARM by considering preferential flow in the porous media. Compared with the ARM, the continuum model underestimated percolation for both bare soil and vegetation-covered soil.

References

Albrecht, B. A., and Benson, C. H. 2001. Effect of desiccation on compacted natural clays. *Journal of Geotechnical and Geoenvironmental Engineering*, 127(1), 67-75.

Albright, W. H., Benson, C. H., Gee, G. W., Abichou, T., Roesler, A. C., and Rock, S. A. 2003. Examining the alternatives. *Civil Engineering*, 73(5), 70-75.

Albright, W. H., Benson, C. H., Gee, G. W., Roesler, A. C., Abichou, T., Apiwantragoon, P., Lyles, B. F., and Rock, S. A. 2004. Field water balance of landfill final covers. *Journal of Environmental Quality*, 33, 2317-2332.

Gee, G. W., Ward, A. L., and Wittreich, C. D. 2002. *The Hanford Site 1000-Year Cap Design Test*. Richland: Pacific Northwest National Lab.

Hangen, E., Gerke, H. H., Schaaf, W., and Hüttl, R. F. 2004. Flow path visualization in a lignitic mine soil using iodine-starch staining. *Geoderma*, 120(1-2), 121-135. [doi:10.1016/j.geoderma.2003.08.011]

Hatano, R., and Booltink, H. W. G. 1992. Using fractal dimensions of stained flow patterns in a clay soil to predict bypass flow. *Journal of Hydrology*, 135(1-4), 121-131. [doi:10.1016/0022-1694(92)90084-9]

Hauser, V. L., Weand, B. L., and Gill, M. D. 2001. Natural covers for landfills and buried waste. *Journal of Environmental Engineering*, 127(9), 768-775. [doi:10.1061/(ASCE)0733-9372(2001)127:9(768)]

Huang, G. H. 1995. Evaporation and crop transpiration under the conditions of the simulation and prediction of soil moisture dynamics. *Journal of Wuhan University of Hydraulic and Electric Engineering*, (10), 55-59. (in Chinese)

Khire, M. V., Benson, C. H., and Bosscher, P. J. 1997. Water balance modeling of earthen final covers. *Journal of Geotechnical and Geoenvironmental Engineering*, 123(8), 744-754. [doi:10.1061/(ASCE) 1090-0241 (1997)123:8(744)]

Khire, M. V., Benson, C. H., and Bosscher, P. J. 2000. Capillary barriers: Design variables and water balance. *Journal of Geotechnical and Geoenvironmental Engineering*, 126(8), 695-708. [doi:10.1061/(ASCE) 1090-0241(2000)126:8(685)]

Liu, H. H., Doughty, C., and Bodvarsson, G. S. 1998. An active fracture model for unsaturated flow and transport in fractured rocks. *Water Resources Research*, 34(10), 2633-2646.

Liu, H. H., Zhang, G. X., and Bodvarsson, G. S. 2003. The active fracture model: Its relation to fractal flow patterns and an evaluation using field observations. *Vadoze Zone Journal*, 2, 259-269.

Lu, J. H., and Wu, L. S. 2003. Visualizing bromide and iodide water tracer in soil profiles by spray methods. *Journal of Environmental Quality*, 32, 363-367.

Melchior, S. 1997. In situ studies on the performance of landfill caps. *Land Contamination Reclamation*, 5, 209-216.

Nyhan, J. W., Hakonson, T. E., and Drennon, B. J. 1990. A water balance study of two landfill cover designs for semiarid regions. *Journal of Environmental Quality*, 19, 281-288.

Nyhan, J. W. 2005. A seven-year water balance study of an evapotranspiration landfill cover varying in slope for semiarid regions. *Vadose Zone Journal*, 4, 466-480. [doi:10.2136/vzj2003.0159]

Olsson, J., Persson, M., Albergel, J., Berndtsson, R., Zante, P., Öhrström, P., and Nasri, S. 2002. Multiscaling analysis and random cascade modeling of dye infiltration. *Water Resources Research*, 38(11), 1263. [doi: 10.1029/2001WR000880]

Sadek, S., Ghanimeh, S., and El-Fadel, M. 2007. Predicted performance of clay-barrier landfill covers in arid and semi-arid environments. *Waste Management*, 27(4), 572-583. [doi:10.1016/j.wasman.2006.06.008]

Scanlon, B. R., Keese, K., Reedy, R. C., Simunek, J., and Andraski, B. J. 2003. Variations in flow and transport in thick desert vadose zones in response to paleoclimatic forcing (0-90 kyr): Field measurements, modeling, and uncertainties. *Water Resources Research*, 39(7), 1179. [doi: 10.1029/2002WR001604]

van Genuchten, M. 1980. Closed-form equation for predicting the hydraulic conductivity of unsaturated soil. *Soil Science Society of America Journal*, 44(4), 892-898.

Vrugt, J. A., Hopmans, J. W., and Simunek, J. 2001. Calibration of a two dimensional root water uptake model. *Soil Science Society of America Journal*, 65(4), 1027-1037.

Wang, K., Zhang, R. D., and Yasuda, H. 2006. Characterizing heterogeneity of soil water flow by dye infiltration experiments. *Journal of Hydrology*, 328(3-4), 559-571. [doi:10.1016/j.jhydrol.2006.01.001]